J Membrane Biol (2014) 247:1229–1237
DOI 10.1007/s00232-014-9736-y

Numerical Modeling of Bi-polar (AC) Pulse Electroporation of Single Cell in Microchannel to Create Nanopores on its Membrane

Saeid Movahed · Yousef Bazargan-Lari · Farhang Daneshmad · Mashhood Mashhoodi

Received: 22 July 2014 / Accepted: 24 September 2014 / Published online: 5 October 2014

Abstract AC electroporation of a single cell in a microchannel was numerically studied. A 15 μm diameter cell was considered in a microchannel 25 μm in height and the influences of AC electric pulse on its membrane were numerically investigated. The cell was assumed to be suspended between two electroporative electrodes embedded on the walls of a microchannel. An amplitude and a time span of applied electric pulse were chosen to be 80 kV/m and 10 μs, respectively. For different frequency values (50, 100, 200, and 500 kHz), simulations were performed to show how the cell membrane was electroporated and the creation of nanopores. Obtained numerical results show that the most and the largest nanopores are created around poles of cell (nearest points of cell membrane to the electrodes). The numerical simulations also demonstrate that increased frequency will slightly decrease electroporated area of the cell membrane; additionally, growth of the created nanopores will be stabilized. It has also been proven that size and number of the created nanopores will be decreased by moving from the poles to the equator of the cell. There is almost no nanopore created in the vicinity of the equator. Frequency affects the rate of generation of nanopores. In case of AC electroporation, creation of nanopores has two phases that periodically repeat over time. In each period, the pore density sharply increases and then becomes constant. Enhancement of the frequency will result in decrease in time span of the periods. In each period, size of the created nanopores sharply increases and then slightly decreases. However, until the AC electric pulse is present, overall trends of creation and development of nanopores will be ascending. Variation of the size and number of created nanopores can be explained by considering time variation of transmembrane potential (difference of electric potential on two sides of cell membrane) which is clear in the results presented in this study.

Keywords Electroporation · Electropermeabilization · Cell · Microchannel · Membrane · AC electric field

S. Movahed (✉)
School of Mechanical Engineering, Amirkabir University of Technology (Tehran Polytechnic), Tehran, Iran
e-mail: smovahed@aut.ac.ir

Y. Bazargan-Lari
Department of Mechanical Engineering, Shiraz Branch, Islamic Azad University, Shiraz, Iran

F. Daneshmad
Department of Mechanical Engineering, McGill University, 817 Sherbrooke Street West, Montreal, QC H3A 2K6, Canada

F. Daneshmad
Department of Bioresource Engineering, McGill University, 21111 Lakeshore Road, Sainte-Anne-de-Bellevue, QC H9X 3V9, Canada

M. Mashhoodi
Department of Management, Science and Technology, Amirkabir University of Technology (Tehran Polytechnic), Tehran, Iran

Introduction

Electric field is usually used in microfluidic biomedical microdevices for different purposes of cell studies such as early diagnostics and treatments of malignant cancer diseases [4, 7, 20, 21, 27] and gene therapy [18]. Presence of the electric field in microchannels can manipulate the cells [10], separate the cells and particles by size [11, 26],

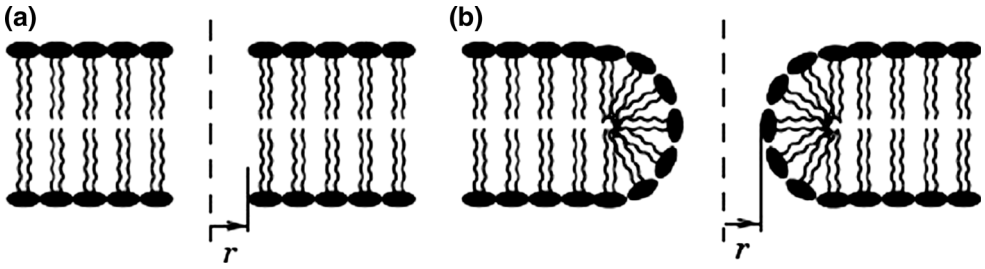

Fig. 1 Schematic diagram of hydrophobic (**a**) hydrophilic (**b**) nanopores. Reprint with permission from [24]

increase the volume of the cell [31], and alter cell membrane structure [21–23]. One of the main influences of the external electric field on the cell membrane is electroporation, synonymously termed electropermeabilization [33]. If the electric potential inside and outside of the cell membrane is expressed as ϕ_{in} and ϕ_{out}, transmembrane potential (ϕ_m), which is the difference of electric potential on two sides of the cell membrane, it will be defined as

$$\phi_m = \phi_{\text{in}} - \phi_{\text{out}} \tag{1}$$

In absence of the external electric field, TMP is equal to rest potential (ϕ_{rest}). The rest potential for Mammalian cells is around -80 mV [17].

Based on the theory of membrane permeabilization, two types of nanopores are created on the cell membrane: hydrophobic and hydrophilic. Fig. 1 depicts a schematic diagram of these kinds of nanopores. The hydrophobic nanopores are gaps in lipid bi-layer of the membrane that are randomly formed by thermal fluctuation. The hydrophilic nanopores have their walls lined with water-attracting heads of lipid molecules. In contrast to the hydrophobic nanopores, the hydrophilic nanopores allow transport of water-soluble substances, such as ions, and thus conduct electric current [24]. Presence of the electric field in the vicinity of the cell membrane alters the transmembrane potential, i.e., the difference of the electric potential on the two sides of the cell membrane. For sufficiently strong electric pulses, the TMP will reach critical value of 0.5–1 V which will significantly disturb the cell membrane structure and create the hydrophobic nanopores on the cell membrane [3, 5]. This effect is usually referred to as electroporation or electropermeabilization. If the properties of electric pulse are controlled accurately (e.g., for DC electric pulse: intensity and duration, and for AC electric pulse: amplitude and frequency), the created nanopores will be hydrophobic, reversible, and will not affect cell viability. These nanopores can be treated as a pathway to insert different types of biological nanoparticles into the cell. The insertion of the biological nanoscale samples, such as DNA and QDots, facilitates early diagnosis and treatment of different diseases such as malignant cancers [21].

The first successful reversible electroporation and DNA electrotransfer was reported in 1982 [25]. Traditional electroporative devices suffer from a lack of highly successful transfection rate[1] and cell viability[2] [15]. Microscale electroporation has the best cell viability and transfection rate compared with its traditional counterparts such as macroscale electroporation devices and chemical reagents [15]. Microfluidic devices offer many advantages such as significant reduction in consumption of chemical reagents and biological samples and provide continuous flow similar to real situation in living biological systems that can deliver nutrients to the cells and remove waste produced by the cells [20].

The idea of performing cell electroporation on microfluidic and lab-on-a-chip devices was initiated at the beginning of this millenium [8, 9]. Since then, many microfluidic lab-on-a-chip devices have been designed for cell electroporation. Readers may consult with the review papers on this topic to become familiar with these experimental studies [21, 29, 32]. Until now, theoretical studies on the microfluidic cell electroporation lag behind the experimental ones though the mathematical modeling and theoretical results are completely essential to boost the current understanding of the cell electroporation, reduce undesired influences of the electric field on the cell membrane, and increase the quality of the reversible cell electroporation (e.g., increase the cell viability and the transfection rate). Some theoretical studies have been conducted on the cell electroporation [14, 30]; however, the findings of many of these studies are not applicable to the microfluidic cell electroporation since they consider the cells in infinite domain which does not reflect boundary effects of the walls of microchannels on the cell electroporation. Some other studies have also been published that consider the cells in various micro-geometries and calculate spatial distribution of the electric field in the vicinity of the cell membrane during electroporation [1, 2, 6, 12, 19], or find the transmembrane potential of the cell [13]. However, these articles do not predict size and number of created nanopores on the cell membrane.

[1] transfection rate is defined as a ratio of number of successfully transfected cells to number of total cells.

[2] cell viability is defined as number of viable cells after performing electroporation to total number of cells.

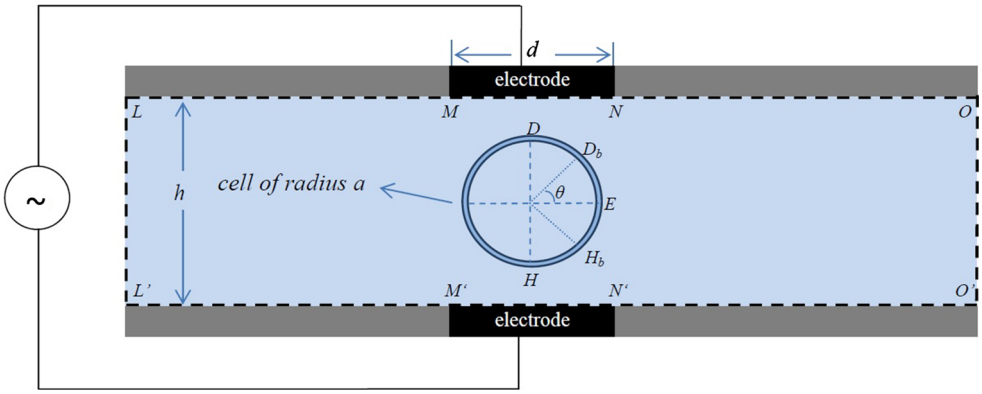

Fig. 2 The schematic diagram of the assumed system of the current study. A cell of radius a is assumed in the microchannel of height h. The microchannel is filled with the conductive medium. An AC electric pulse ($\phi_0 \sin(\omega t)$) is applied via the two electrodes located on the wall of the microchannel

One of the first theoretical studies on the cell electroporation in the microchannels was conducted by Movahed and Li [23] in 2012. They assumed that the electrodes were embedded at the walls of the microchannels. This study revealed many aspects of the microfluidic cell electroporation. As an example, their results showed that in the microfluidic systems, the membrane permeabilization can be performed with very low-intensity electric field (1–3 V). The required electric pulse intensity decreases by reducing the size of the microchannel. If the embedded electrodes are larger than the cell diameter, the transmembrane potential becomes less widely spread; by decreasing the size of the electrodes lower than the cell diameter, the local transmembrane potential decreases everywhere and sharply in the area from the poles (the nearest point of the cells to the electrodes) to the equator. Their results also indicate that the number of created nanopores reaches its maximum value extremely fast; further presence of the electric pulse may no longer influence the number and location of the created nanopores. It only develops the generated nanopores. The most (fewest) nanopores are created around the poles (equators). This study focused on the DC electroporation of the cells in microchannels though the AC electroporation which is also of interest in the microfluidic devices [16, 28, 29]. Replacing the DC by AC electric pulse results in reduction in bubble generation and pH change in vicinity of the cell membrane [21].

In the current study, we numerically investigate how the AC electric pulses electroporate single cell in the microchannels. The way in which the frequency of AC electric pulse affects location, number, size, and time evaluation of created nanopores is examined. The rest of this article is organized as follows: the next section explains the assumed model of the current study. After that, the mathematical modeling and the governing equations are introduced (see "Mathematical Modeling" section). Then, the used numerical model is explained ("Numerical Simulation" section). The results of the current study are presented and discussed in "Results and Discussion" section. The concluding remarks are provided at the end of this article.

Model Description

Figure 2 schemes the assumed model of the current study. In this study, a spherical cell of radius a (diameter d_0) and membrane thickness of t is assumed. The cell is suspended in the microchannel of height h. Two embedded electrodes on the side wall of the microchannels apply the required electric pulse for electroporation (ϕ).

In this study, the AC electric pulse of intensity ϕ_0 and frequency ω is applied in the vicinity of the cell membrane:

$$\phi = \phi_0 \sin(\omega t) \tag{2}$$

Five points are defined on the cell membrane (see Fig. 2; nearest points on the cell membrane to the electrodes are defined as depolarized (D) and hyperpolarized (H) poles, E represents the equator line, the border between the electroporated and the non-electroporated regions on the membrane is marked as D_b and H_b. The assumed values and parameters of the current study are listed in Table 1.

In the current study, we study how the AC electric pulse creates the hydrophilic nanopores on the cell membrane. Based on the theory of membrane permeabilization, the created nanopores on the cell membrane are initially hydrophobic. When the transmembrane potential reaches the critical values of 0.5–1 V, the hydrophobic nanopores will convert to the hydrophilic. The threshold radius whereby the hydrophobic nanopores convert to the hydrophilic ones is $r^* = 0.51$ nm. In the theory of membrane permeabilization, the energy concept was utilized to develop a mathematical model of the cell membrane permeabilization in terms of a set of partial differential equations (PDE) [24]. Because of the presence of disparate spatial and temporal scales, it is difficult to numerically solve this set of partial differential equations. In 1999, Neu and Krassowska proposed an asymptotic reduction of the set of partial equations to an ordinary differential equation (ODE) which is easier to solve by numerical methods [24]. In the present investigation, this

Table 1 The values for constants and parameters used in this study

Parameter	Value/range (unit)	Definition
d_0	15 μm	Diameter of the cell
a	7.5 μm	Radius of the cell
h_c	5 nm	Membrane thickness
h	25 μm	Height of the microchannel
d	20 μm	Size of the electrodes
ϕ_0	1, 1.5, 2, 2.5 (V)	Amplitude
f	50, 100, 200, 500 kHz	Frequency
t	10 μs	Time
s_i	0.455	Interacellular conductivity
s_e	5	Extracellular conductivity
s	2	Conductivity of the solution filling the nanopore
C_m	0.0095	Surface capacitance
g_1	2	Surface conductance
V_{rest}	−80 (mV)	Rest potential
α	1×10^9	Constant used in Eq. 15
V_{ep}	0.258	Constant used in Eqs. 15 and 17
N_0	1×10^9	Constant used in Eq. 17
r^*	0.51	Threshold radius of hydrophobic and hydrophilic nanopores
D	5×10^{-14}	Diffusion coefficient
k	1.38065×10^{-23} (m^2 kg/(s^2 K))	Boltzmann constant
T	300 K	Temperature
β	1.4×10^{-19} (J)	Constant used in Eq. 13
γ	1.8×10^{-11} (J/m)	Constant used in Eq. 13
F_{max}	0.7×10^{-9} (Number/r^2)	Constant used in Eq. 13
r_h	0.97×10^{-9} (m)	Constant used in Eq. 13
r_t	0.31×10^{-9} (m)	Constant used in Eq. 13
q	$(r_m/r*)^2$	Constant used in Eq. 17
σ'	2×10^{-2} (J/m^2)	Constant used in Eq. 14
σ_0	1×10^{-6} (J/m^2)	Constant used in Eq. 14

ODE model is applied to the cell located in the microchannel to study how the AC electric pulse electroporate the cell membrane.

Mathematical Modeling

As it was indicated before, the ODE equations proposed by Neu and Krassowska [24] are utilized to model the AC electroporation of the cell in the microchannel. In the following sections, a brief review of this method will be explained.

Electric Field

The Laplace equation should be solved to find the interacellular (ϕ_i) and extracellular (ϕ_e) electric potentials:

$$\nabla^2 \phi_{i,e} = 0 \tag{3}$$

The two embedded electrodes on the two sides of the cell apply the required voltage of electroporation to the cell membrane ($\phi_0 \sin(\omega t)$). To consider the effect of applied voltage in the simulations, the following mathematical conditions are assumed on boundaries MN and M_0N_0:

$$\phi_{e,MN} = \phi_0/2\sin(\omega t) \tag{4}$$

$$\phi_{e,MN} = -\phi_0/2\sin(\omega t) \tag{5}$$

The walls of microchannel are electrically insulated. There is also no current flow at the two ends of the microchannel. Therefore, the assumed electrical condition on boundaries $LM, NO, OO', O'N', M'L'$, and $L'L$ is

$$\hat{n}.\mathbf{J} = 0 \tag{6}$$

The electric current density should be continuous across the cell membrane:

$$-\hat{n}.(s_i \nabla \phi_i) = -\hat{n}.(s_e \nabla \phi_e) = c_m \frac{\partial V_m}{\partial t} + g_1(V_m - V_{rest}) + I_p \tag{7}$$

In the above equations, $\mathbf{J}$ is the current density, $\hat{n}$ the local outward unit vector normal to the surface of cell membrane, ∇ the Nabla symbol, s_i and s_e the interacellular and extracellular conductivities, V_m and V_{rest} the transmembrane and rest potentials, and g_1 and c_m are the surface conductance and capacitance of the membrane, in that order. In this equation, the transmembrane potential can be found by solving Eq. 1.

First and second terms of right-hand side of Eq. 7 represent capacitive current ($\frac{\partial V_m}{\partial t}$) and current through the protein channels ($g_1(V_m - V_{rest})$, respectively. I_p represents current through the created nanopores. If the cell membrane is discretized into k elements, surface area of each segment can be found as $\delta A = 2\pi a/k$. At each of these sections of membrane, I_p can be found as

$$I_p(t) = \frac{1}{\nabla A} \Sigma_{j=1}^{m} i_p(r_j, V_m) \tag{8}$$

Here, m is the number of created nanopores at each segment and i_p is the current through each nanopore, that can be computed using the following equation:

$$i_p(r, V_m) = \frac{V_m}{R_p + R_i} \tag{9}$$

where R_p is the ohmic resistance of the cylindrical pores and R_i is the correcting resistance that is used to consider the effect of changing TMP in the vicinity of the pores:

$$R_p = \frac{h}{s\pi r^2} \tag{10}$$

$$R_i = \frac{1}{2sr} \tag{11}$$

In the above equations, h and s are the membrane thickness and conductivity of the solution filling the nanopore, respectively.

Radius of Nanopores

The ODE asymptotic model proposed by Neu and Krassowska [24] is based on the assumption that the nanopores are initially created hydrophilic with a radius of r^*. By increasing the applied electric field, the nanopores start to develop in order to minimize energy of the cell membrane. If the number of the created nanopores is n, the rate of variation of their radii, r_j, can be determined by the following set of equations:

$$\frac{dr_j}{dt} = U(r_j, V_m, \sigma_{\text{eff}}), \quad j = 1, 2, ..., n \tag{12}$$

$$U(r, V_m, \sigma_{\text{eff}}) = \frac{D}{kT} 4\beta \left(\frac{r_*}{r}\right)^4 \frac{1}{r} - 2\pi\gamma + 2\pi\sigma_{\text{eff}} r + \frac{V_m^2 F_{\max}}{1 + r_h/(r + r_t)} \tag{13}$$

The constants of the above equations are defined in Table 1. σ_{eff} is the effective tension of the membrane. If A is the surface area of the cell membrane and A_p is the area of the created nanopores ($A_p = \Sigma_{i=1}^{n} \pi r_i^2$), σ_{eff} can be computed as

$$\sigma_{\text{eff}}(A_p) = 2\sigma' - \frac{2\sigma' - \sigma_0}{(1 - A_p/A)^2} \tag{14}$$

Number of Nanopores

The rate of creation of nanopores can be found as

$$\frac{dN(t)}{dt} = \alpha e^{(V_m/V_{ep})^2} \left(1 - \frac{N(t)}{N_{ep}(V_m)}\right) \tag{15}$$

where $N(t)$, density of pores, is defined as

$$N(t) = \int_{r^*}^{\infty} n(r, t) \mathrm{d}r \tag{16}$$

N_{ep} is the equilibrium pore density for the given transmembrane voltage (V_m) which can be calculated as

$$N_{ep}(V_m) = N_0 e^{q(V_m/V_{ep})^2} \tag{17}$$

In the above equations, α, V_{ep}, q, and N_0 are the constants and are shown in Table 1.

Numerical Simulation

In this study, the above-mentioned governing equations were solved numerically to find the electric potential in the domain and to investigate how the AC electric pulse electroporate the cell membrane. The Comsol3.5a (http://www.comsol.com/) commercial package along with Matlab was used in the numerical simulations. The cell membrane was discretized with a discretization step of $\delta\theta = \pi/60$. In order to discretize the solution domain, unstructured meshes were applied. The solution domain was broken into small meshes to allow them to fully cover the solution domain without overlapping. At the initial state and before applying the electric pulse, TMP was equal to the rest potential ($V_m = V_{\text{rest}}$). At each time step, Eqs. 3–7 were solved by the finite element method in Comsol3.5a to find the electric potential in the domain. After the electric potential was obtained, Eqs. 8–17 were solved by Matlab to find the location, number, and radius of the created nanopores on the membrane. The 'Runge Kutta' method was utilized to solve ODE Eqs. 12 and 15. This system of equations was solved with a time step of 0.02 μs.

Results and Discussion

In this section, for one specific case of study, the way in which AC electric pulse will electroporate a single cell located in microchannel was investigated. The assumed constants and parameters of this study have been presented in Table 1. The cell of radius a (7.5 μm) is considered in the microchannel of height h (25 μm). A necessary electric pulse of electroporation is applied by two electrodes of width d located on walls of the microchannel. The pulse shape is chosen as a sinusoidal wave (AC electric pulse) that can be mathematically expressed as $\phi = \phi_0 \sin(\omega t)$. The electric pulse span is in the order of microseconds. In this section, we present the influence of electric pulse frequency (f) on quality of cell membrane permeabilization. For DC electroporation, the effects of geometrical parameters, such as height of the channel and size of electrode, which should be the same for AC

electroporation, have been investigated in the article published by the same author in 2013 [23].

Radius of Created Nanopores

In the asymptotic model of membrane permeabilization, it is assumed that the nanopores are initially created as hydrophilic with radius of $r^* = 0.51\,\text{nm}$ [24]. In this section, the way in which the radius of created nanopores is developed over time is investigated. The amplitude of applied electric pulse is equal to 80 kV/m.

It should be mentioned that number density and radius of the created nanopores will be symmetric along the equator[3] and poles of the cell.[4] This is because all the electrical and geometrical parameters are symmetric along these two lines (see Fig. 2). Thus, in the current study, only the results on the quarter of the cell membrane ($0^\circ < \theta < 90^\circ$) are illustrated.

For two different frequencies, 100 and 500 kHz, Fig. 3 depicts how the created nanopores on cell membrane expand over time. Firstly, this figure shows that the largest nanopores are mainly created around the poles of the cell membrane (points D and H that have angular positions of $\theta = 90^\circ$ and 270°, respectively). This figure also demonstrates how different frequencies of applied AC electric pulse affect the size of created nanopores on different angular positions of the cell membrane. In this figure, the amplitude of the applied electric pulse is equal to 80 kV/m and the frequencies are 100 (Fig. 3a) and 500 kHz (Fig. 3b), respectively. Increase of the frequency will slightly decrease the electroporated area of the cell membrane.

Development of the created nanopores will also be influenced by frequency. It is better illustrated in Fig. 4. For two different angular positions of the cell membrane, this figure demonstrates how different frequencies of applied electric field impact developments of the created nanopores. This figure also shows that the largest nanopores will be created around the poles ($\theta = 90^\circ$). Furthermore, it implies that increase of the frequency of applied AC electric pulse will stabilize the growth of the created nanopores. Larger frequencies cause less fluctuations in growth of the created nanopores on the cell membrane.

To recap, it can be concluded that by keeping the amplitude of applied electric pulse constant, enhancement of the frequency of applied electric field, on the one hand, will stabilize the growth of nanopores and, on the other hand, will narrow the electroporated area of the cell membrane. In addition, by going from the poles ($\theta = 90^\circ$ and 270°) to the equator of the cell membrane ($\theta = 0^\circ$ and 180°), the size of created nanopores decreases. There are almost no nanopores near the equator of the cell.

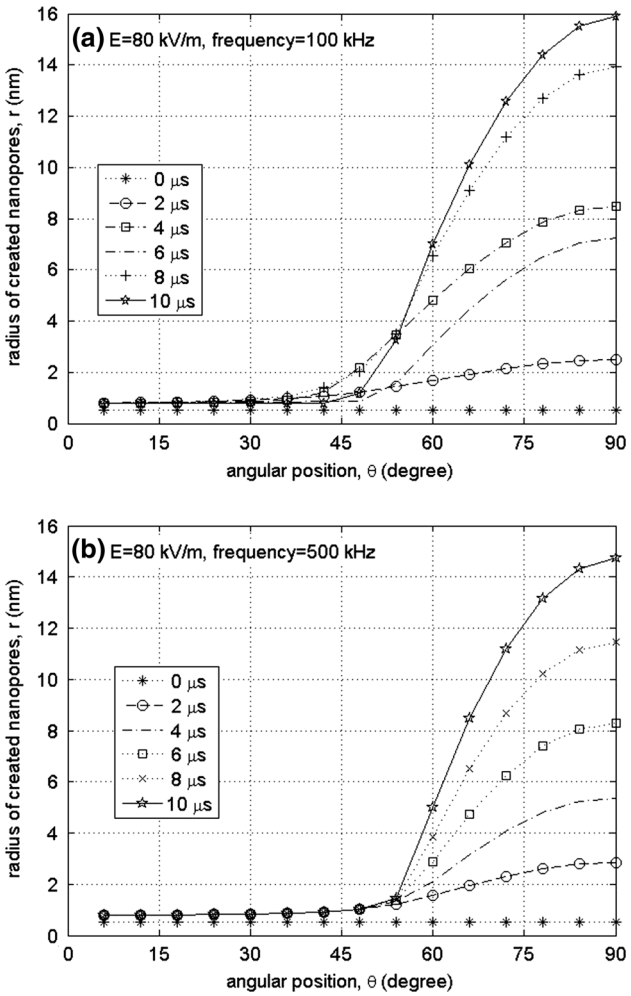

Fig. 3 For two different frequencies 100 kHz (**a**) and 500 kHz (**b**), this figure shows how the created nanopores at each point of the cell membrane develop over time. The assumed applied electric field is 80 kV/m

Number Density of Created Nanopores

As previously mentioned, this article only depicts the results at the quarter of the cell membrane ($0^\circ < \theta < 90^\circ$). This is because of symmetry along the equator and imaginary vertical line passing through DH (see Fig. 2). Figure 5 shows how the frequency of applied electric pulse influences creation of nanopores. From this figure, it can be implied that, first, the nanopores are mainly created around the poles. By going from the poles toward the equator, the nanopores are rarely created; there are no nanopores around the equator. Secondly, frequency has less influence on the number and location of created nanopores. In Fig. 5a, b frequency is 100 and 500 kHz, respectively.

[3] an imaginary line drawn around the cell equally distant from both poles, dividing the cell into northern and southern hemispheres.

[4] will be defined as nearest and farthest points of the cell membrane to the electrodes (D and H).

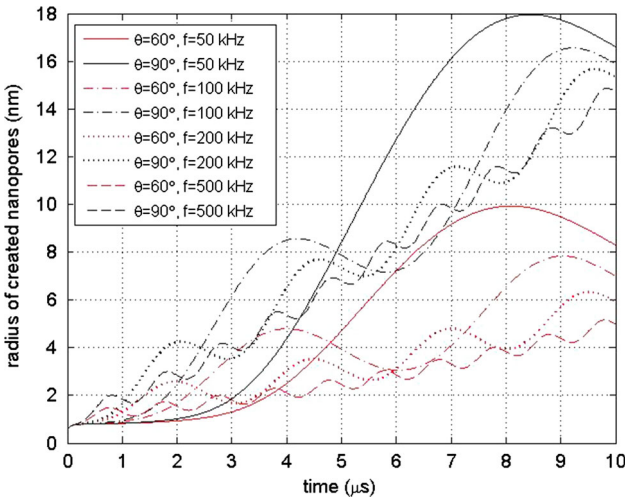

Fig. 4 For two different angular positions on cell membrane ($\theta = 60°$ and 90°), this figure shows how the radius of created nanopores develops for different assumed values of frequencies (50, 100, 200, and 500 kHz). Amplitude of applied AC electric field is assumed to be 80 kV/m

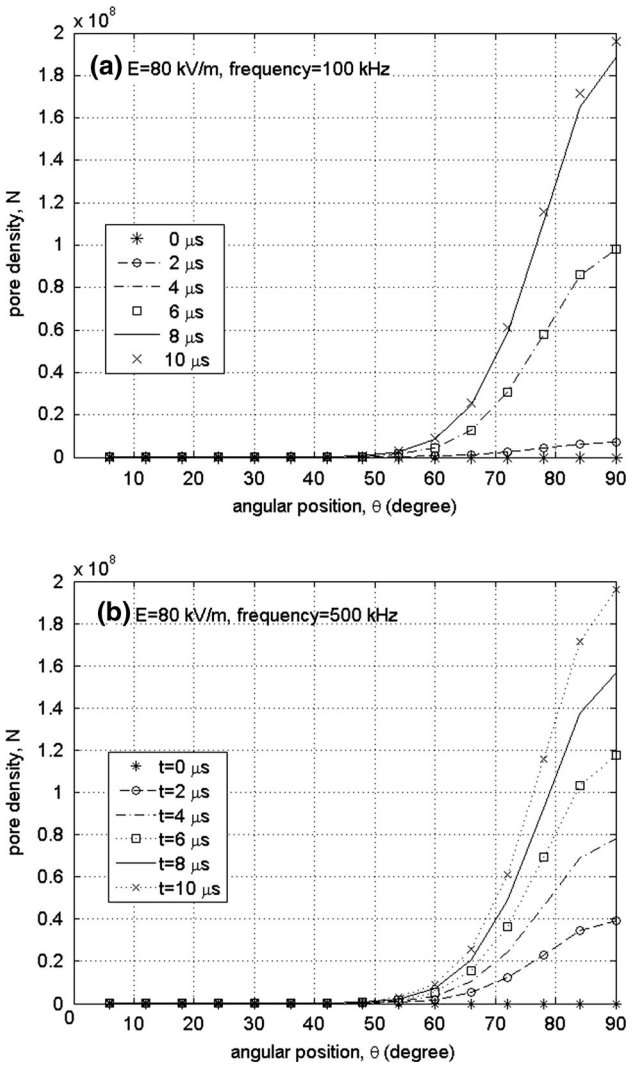

Fig. 5 For two different frequencies, 100 kHz (**a**) and 500 kHz (**b**), this figure shows how the number of created nanopores around the cell membrane increases over time. The assumed applied electric field is 80 kV/m

However, there are no any substantial differences between the number and the location of created nanopores. It just affects rate of creation of nanopores. This can be explained by considering Fig. 6. For two different angular positions on the cell membrane ($\theta = 60°$ and 90°), this figure depicts how the frequency of applied electric pulse affects creation of nanopores. It has less impact on the number of created nanopores; however, it mostly influences rate of generation of nanopores. This figure shows that in the case of AC electroporation, creation of nanopores has two phases that are periodically repeated over time. In each period, the pore density sharply increases and then becomes constant. For higher frequency values, time span of each period decreases and the time evaluation of creation of nanopores will approach to linear behavior. Figure 6 also indicates that pore density at poles is almost twice more than angular position $\theta = 60°$.

Transmembrane Potential

Driving force of creation of nanopores on cell membrane is induced transmembrane potential. Transmembrane potential is defined as difference of electric potential at two sides of the cell membrane. The presence of an external electric field in the vicinity of the cell membrane alters TMP and induce excess energy to the cell membrane. Nanopores will be created on the cell membrane to reduce level of energy. Indeed, they act as a sink of energy to absorb the induced energy to the cell.

As it was demonstrated in the previous sections, the most and biggest nanopores will be created around the poles; thus, in this section, without loss of generality, it is explained how the frequency of applied electric pulse influences the induced transmembrane potential at the poles ($\theta = 90°$). Figure 7 depicts time variation of transmembrane potential at this angular position. Increase of the frequency will intensify fluctuation of the transmembrane potential. As an example, for $f = 100\,\text{kHz}$, it takes 5 s for the TMP to complete one cycle. However, for the same period of time, the TMP completes 2.5 cycles when the frequency is kept to 500 kHz,.

Development of size and number of the created nanopores can be explained by considering time variation of the transmembrane potential. The created nanopores on cell membrane are initially hydrophobic. When the TMP reach to the critical value of 0.5–1 V, the hydrophobic

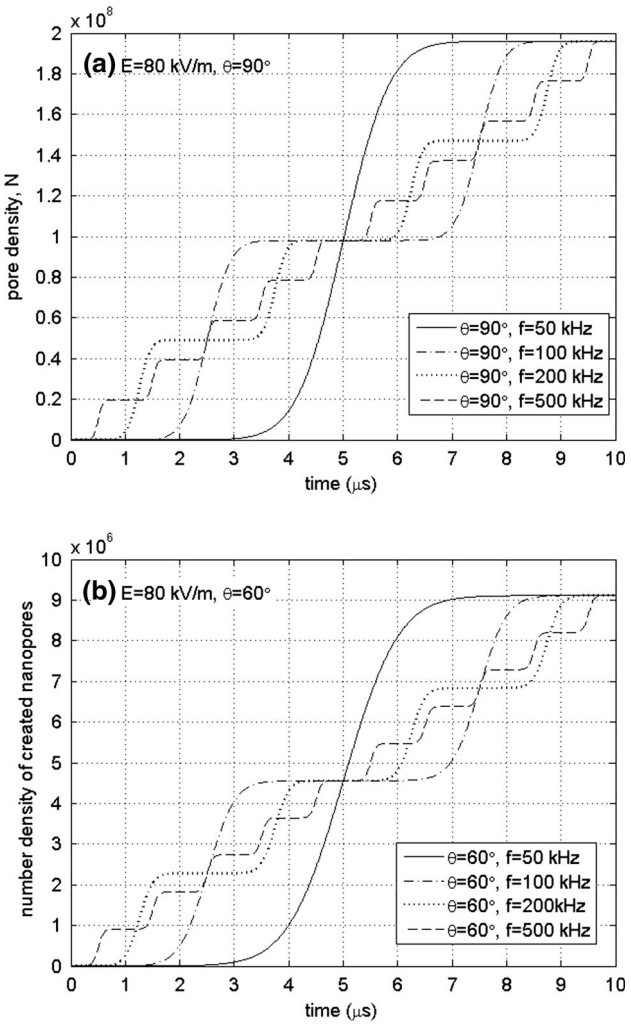

Fig. 6 At two different angular positions $\theta = 90^\circ$ (**a**) and $\theta = 60^\circ$ (**b**), this figure shows how the frequency of applied electric pulse influences creation of the nanopores. The assumed applied electric field is 80 kV/m

nanopores turn into hydrophilic ones; further presence of this TMP will cause creation and development of hydrophilic nanopores [21, 24]. In AC-electroporation, if the pulse intensity is high enough to generate hydrophilic nanopores on the cell membrane, the TMP is not always greater than the critical value of 0.5–1 V; this is because of the sinusoidal nature of applied electric field. In each cycle, when the TMP is larger than this critical value, the nanopores will start to create and develop; however, number and radius of the created nanopores will be decreased during the rest of the period in which TMP is lower than the critical value. It causes fluctuations in creation and development of the nanopores. Time interval of these fluctuations is consistent with the frequency of applied electric pulses. As an example, see Figs. 4, 6, and 7.

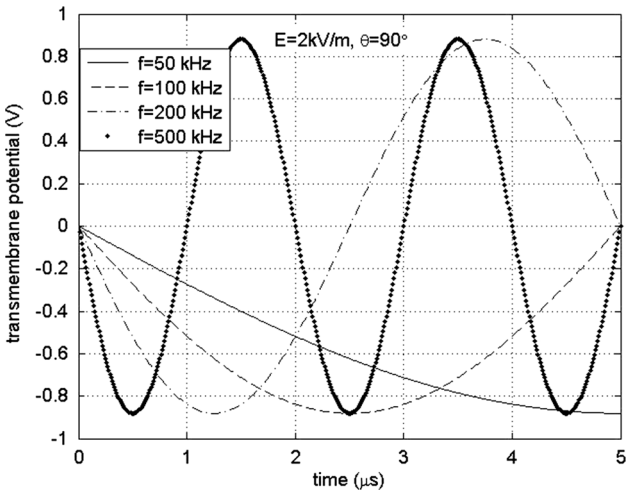

Fig. 7 This figure illustrates how the frequency of applied electric pulse affects the induced transmembrane potential at the pole of the cell membrane ($\theta = 90^\circ$). Amplitude of the applied electric pulse is 2 kV/m

Concluding Remarks

Presence of a sufficiently high electric pulse near cell membrane can significantly disturb the cell membrane structure and create hydrophilic nanopores on it. This effect is usually referred to electroporation (or electropermeabilization). If the applied electric pulse is controlled accurately, the created nanopores will be reversible and will not affect cell viability. Different biological nanoparticles, such as DNA and QDots, can be inserted into the cell via these created nanopores. Performing cell electroporation in microfluidic systems will provide feasibility of online monitoring, single-cell study, and high viability and transfection rate. Replacing DC with AC electric pulse results in reduction in bubble generation and pH change in vicinity of the cell membrane. It will cause fewer damages to the structure of cell membrane. In this article, a numerical modeling has been performed on AC electroporation of cell in microchannels. Obtained numerical results show that the most and the largest nanopores are created around the poles of cell (the nearest points of cell membrane to the electrodes). It was concluded that size and number of created nanopores decreased by moving from the poles to the equator of the cell. There were almost no nanopores created in the vicinity of the equator (an imaginary line drawn around the cell equally distant from both poles, dividing the cell into northern and southern hemispheres). These numerical findings are qualitatively in line with the membrane permeabilization of the cells in the infinite domain. The numerical results also show that increase of the frequency would slightly decrease the

electroporated area of the cell membrane. Higher frequencies also stabilize growth of created nanopores. Frequency, too, affects rate of generation of nanopores. In case of AC electroporation, creation of nanopores has two phases that are periodically repeated over time. In each period, the pore density sharply increases and then becomes constant. Enhancement of frequency causes reduction in time span of these periodic phases. In each period, size of the created nanopores sharply increases and then slightly decreases. However, as long as the electric pulse is present, the overal trend of creation and development of nanopores will be upward. Variation of the size and number of created nanopores can be explained by considering time variation of transmembrane potential (difference of electric potential on two sides of cell membrane) which is the reason of cell membrane permeabilization.

References

1. Adamo A, Arione A, Sharei A, Jensen KF (2013) Flow-through comb electroporation device for delivery of macromolecules. Anal Chem 85(3):1637–1641
2. Cemazar J, Vrtacnik D, Amon S, Kotnik T (2011) Dielectrophoretic field-flow microchamber for separation of biological cells based on their electrical properties. NanoBioscience 10(1):36–43
3. Chang DC, Chassy BM, Saunders JA, Sowers AE (1992) Guide to electroporation and electrofusion. Access Online via Elsevier
4. Geng T, Lu C (2013) Microfluidic electroporation for cellular analysis and delivery. Lab Chip 13(19):3803–3821
5. Ho S, Mittal G, Cross J (1997) Effects of high field electric pulses on the activity of selected enzymes. J Food Eng 31(1):69–84
6. Hu N, Yang J, Yin ZQ, Ai Y, Qian S, Svir IB, Xia B, Yan JW, Hou WS, Zheng XL (2011) A high-throughput dielectrophoresis-based cell electrofusion microfluidic device. Electrophoresis 32(18):2488–2495
7. Hu N, Zhang X, Yang J, Joo SW, Qian S (2013) A cell electrofusion microfluidic chip with micro-cavity microelectrode array. Microfluid Nanofluid 15(2):151–160
8. Huang Y, Rubinsky B (2001) Microfabricated electroporation chip for single cell membrane permeabilization. Sens Actuators A 89(3):242–249
9. Huang Y, Rubinsky B (2003) Flow-through micro-electroporation chip for high efficiency single-cell genetic manipulation. Sens Actuators A 104(3):205–212
10. Kang Y, Li D (2009) Electrokinetic motion of particles and cells in microchannels. Microfluid Nanofluid 6(4):431–460
11. Kang Y, Li D, Kalams SA, Eid JE (2008) Dc-dielectrophoretic separation of biological cells by size. Biomed Microdevices 10(2):243–249
12. Kim SK, Kim JH, Kim KP, Chung TD (2007) Continuous low-voltage dc electroporation on a microfluidic chip with polyelectrolytic salt bridges. Anal Chem 79(20):7761–7766
13. Kotnik T, Pucihar G, Miklavčič D (2010) Induced transmembrane voltage and its correlation with electroporation-mediated molecular transport. J Membr Biol 236(1):3–13
14. Krassowska W, Filev PD (2007) Modeling electroporation in a single cell. Biophys J 92(2):404–417
15. Lee WG, Demirci U, Khademhosseini A (2009) Microscale electroporation: challenges and perspectives for clinical applications. Integr Biol 1(3):242–251
16. Lim JK, Zhou H, Tilton RD (2009) Liposome rupture and contents release over coplanar microelectrode arrays. J Colloid Interface Sci 332(1):113–121
17. Lodish H (2008) Molecular cell biology. Macmillan, New York
18. Longsine-Parker W, Wang H, Koo C, Kim J, Kim B, Jayaraman A, Han A (2013) Microfluidic electro-sonoporation: a multimodal cell poration methodology through simultaneous application of electric field and ultrasonic wave. Lab Chip 13(11):2144–2152
19. MacQueen LA, Buschmann MD, Wertheimer MR (2008) Gene delivery by electroporation after dielectrophoretic positioning of cells in a non-uniform electric field. Bioelectrochemistry 72(2):141–148
20. Movahed S, Li D (2010) Numerical studies of continuous nutrient delivery for tumour spheroid culture in a microchannel by electrokinetically-induced pressure-driven flow. Biomed Microdevices 12(6):1061–1072
21. Movahed S, Li D (2011) Microfluidics cell electroporation. Microfluid Nanofluid 10(4):703–734
22. Movahed S, Li D (2013) Electrokinetic transport of nanoparticles to opening of nanopores on cell membrane during electroporation. J Nanopart Res 15(4):1–17
23. Movahed S, Li D (2013) A theoretical study of single-cell electroporation in a microchannel. J Membr Biol 246(2):151–160
24. Neu JC, Krassowska W (1999) Asymptotic model of electroporation. Phys Rev E 59(3):3471–3482
25. Neumann E, Schaefer-Ridder M, Wang Y, Hofschneider P (1982) Gene transfer into mouse lyoma cells by electroporation in high electric fields. EMBO J 1(7):841
26. Nosrati R, Vollmer M, Eamer L, Zeidan K, San Gabriel MC, Zini A, Sinton D (2012) Microfluidic separation of motile sperm with millilitre-scale sample capacity. Bull Am Phys Soc 57
27. del Rosal B, Sun C, Loufakis DN, Lu C, Jaque D (2013) Thermal loading in flow-through electroporation microfluidic devices. Lab Chip 13(15):119–127
28. Sedgwick H, Caron F, Monaghan P, Kolch W, Cooper J (2008) Lab-on-a-chip technologies for proteomic analysis from isolated cells. J R Soc Interface 5(Suppl 2):S123–S130
29. Talele S, Talele S (2013) Drug delivery by electroporation. In: Tarek S, Khaled E (eds) Emerging trends in computing, informatics, systems sciences, and engineering. Springer, Berlin
30. Talele S, Gaynor P, Cree MJ, Van Ekeran J (2010) Modelling single cell electroporation with bipolar pulse parameters and dynamic pore radii. J Electrostat 68(3):261–274
31. Wang HY, Lu C (2006) High-throughput and real-time study of single cell electroporation using microfluidics: effects of medium osmolarity. Biotechnol Bioeng 95(6):1116–1125
32. Wang M, Orwar O, Olofsson J, Weber SG (2010) Single-cell electroporation. Anal Bioanal Chem 397(8):3235–3248
33. Weaver JC, Chizmadzhev YA (1996) Theory of electroporation: a review. Bioelectrochem Bioenerg 41(2):135–160